Scientific Research Publishing

Open Journal of Statistics, 2023, 13, 761-768
https://www.scirp.org/journal/ojs
ISSN Online: 2161-7198
ISSN Print: 2161-718X

Harmonicity Spectrum

Lintao Liu[1], Guocheng Wang[1], Xiaoqing Su[2], Xuepeng Sun[1], Huiwen Hu[1], Xiaowen Luo[3]

[1]The State Key Laboratory of Geodesy and Earth's Dynamics, Innovation Academy for Precision Measurement Science and Technology, Chinese Academy of Sciences, Wuhan, China
[2]Shandong University of Technology, Zibo, China
[3]Key Laboratory of Submarine Geosciences, Second Institute of Oceanography, Ministry of Natural Resources, Hangzhou, China
Email: llt@asch.whigg.ac.cn., guocheng96@apm.ac.cn, sxq_azj@163.com, sunxuepeng@apm.ac.cn, huhuiwen@apm.ac.cn, huhuiwen@apm.ac.cn

How to cite this paper: Liu, L.T., Wang, G.C., Su, X.Q., Sun, X.P., Hu, H.W. and Luo, X.W. (2023) Harmonicity Spectrum. *Open Journal of Statistics*, **13**, 761-768.
https://doi.org/10.4236/ojs.2023.135037

Received: September 13, 2023
Accepted: October 27, 2023
Published: October 30, 2023

Abstract

Perceiving harmonic information (especially weak harmonic information) in time series has important scientific and engineering significance. Fourier spectrum and time-frequency spectrum are commonly used tools for perceiving harmonic information, but they are often ineffective in perceiving weak harmonic signals because they are based on energy or amplitude analysis. Based on the theory of Normal time-frequency transform (NTFT) and complex correlation coefficient, a new type of spectrum, the Harmonicity Spectrum (HS), is developed to perceive harmonic information in time series. HS is based on the degree of signal harmony rather than energy or amplitude analysis, and can therefore perceive very weak harmonic information in signals sensitively. Simulation examples show that HS can detect harmonic information that cannot be detected by Fourier spectrum or time-frequency spectrum. Acoustic data analysis shows that HS has better resolution than traditional LOFAR spectrum.

Keywords

Normal Time-Frequency Transform, Complex Correlation Coefficient, Harmonicity Spectrum, Weak Harmonic Signal Detection

1. Introduction

Fourier transform [1] and time-frequency transform [2] [3] are commonly used tools for perceiving harmonic sub-signals in time series. However, since Fourier spectrum and time-frequency spectrum analysis are based on signal energy or amplitude, they often encounter difficulties in detecting weak harmonic sub-signals, especially in the presence of strong noise. For example, in passive detection of underwater targets, LOFAR spectrum is commonly used to perceive target line

spectra [4]. Since LOFAR spectrum is based on Fourier transform, on the one hand, it is often affected by noise interference, making the spectrum messy; on the other hand, the resolution of LOFAR spectrum is not high enough and its clarity is often not high enough as well. Other classic methods for perceiving harmonic signals, such as correlation and statistical methods [5] [6], are also based on signal energy analysis, and face same difficulties in perceiving low-energy harmonic signals.

This study is based on the theory of Normal time-frequency transform (NTFT) [7] [8] and complex correlation coefficient to develop a new type of spectrum, the Harmonicity Spectrum (HS), to perceive harmonic information in time series, especially weak harmonic information. Compared with Fourier spectrum and time-frequency spectrum, HS has strong perceptual ability for weak harmonic signals; compared with LOFAR spectrum, HS has good clarity and sensitivity. The reason for these advantages is that HS analysis is based on the degree of signal harmony rather than energy or amplitude.

2. Harmonicity Spectrum

HS reflects the intrinsic degree of harmony of a time series, and we can perceive the presence or absence of harmonic signals based on this degree. The determination of HS of a time series $f(t)$ is equivalent to measuring the complex correlation coefficient between its NTFT and the unit harmonic function.

2.1. Normal Time-Frequency Transform

Normal Time-Frequency Transform (NTFT) is the normalized form of linear time-frequency transform. It unifies the three classical transforms in the field of time-frequency analysis, namely short-time Fourier transform, wavelet transform, and S-transform, and unifies their inverse transforms. NTFT has been widely applied in many fields such as oceanic tides [9] [10], Earth rotation [11] [12], Global Position System (GPS) [13], Inertial Navigation System (INS) [14] and so on.

For a time function $f(t) \in C$ in the real domain, its linear time-frequency transform

$$\Psi f(\tau,\varpi) = \int_R f(t)\overline{\psi(t-\tau,\varpi)}\mathrm{d}t,\ \tau,\varpi \in R \tag{1}$$

is called its NTFT if the kernel function $\psi(t)$ satisfies

$$\begin{cases} \hat{\psi}(\omega,\varpi) = 1, & \text{when } \omega = \varpi \\ \left|\hat{\psi}(\omega,\varpi)\right| < 1, & \text{when } \omega \neq \varpi \end{cases} \tag{2}$$

where "^" represents the Fourier operator, overline "-" represents the conjugate, and "$|\bullet|$" represents modulus.

NTFT has an interesting property, namely Inaction principle: for a harmonic signal

$$h(t) = A\exp(i\beta t) = |A|\exp\left(i(\beta t + \Delta)\right) \tag{3}$$

where A represents the complex amplitude, $\beta \in R$ represents the frequency, and $\Delta \in [0, 2\pi]$ represents the initial phase, we have

$$\begin{cases} \left|\Psi h(\tau, \varpi)\right| = Max = \left|h(\tau)\right| \Leftrightarrow \varpi = \beta, & \forall \tau \in R \\ \Psi h(\tau, \beta) = h(\tau), & \forall \tau \in R \end{cases} \tag{4}$$

where " $\Leftrightarrow$ " represents "if and only if", and " $\forall$ " represents "for any". The Inaction principle means that NTFT can directly perceive a harmonic signal without inverse transform. The Inaction principle in fact manifests NTFT's harmonic invariance. Such harmonic invariance can be used to develop the HS to perceive harmonic information in time series based on signal harmony degree, and has better performance than other methods based on signal amplitude or energy analysis.

2.2. Complex Correlation Coefficient

For complex time series $z_1(t)$ and $z_2(t)$, there are two ways to define their correlation coefficient. The first one is given by equation

$$\rho = \frac{\left|\int_D z_1(t)\overline{z_2}(t)\mathrm{d}t\right|}{\sqrt{\int_D \left|z_1(t)\right|^2 \mathrm{d}t \int_D \left|z_2(t)\right|^2 \mathrm{d}t}} \tag{5}$$

and the second one is given by equation

$$\gamma = \frac{\left|\int_D z_1(t)\overline{z_2}(t)\mathrm{d}t\right|}{\int_D \left|z_1(t)\right| \cdot \left|z_2(t)\right| \mathrm{d}t} \tag{6}$$

where D represents the integration time interval. It can be verified that the correlation coefficient takes values in the range [0, 1]. Moreover, when $z_1(t)$ and $z_2(t)$ are harmonic signals with the same frequency, their correlation coefficient is equal to 1. The first definition is useful for suppressing interference, while the second definition is useful for highlighting harmonic information.

2.3. Definition of HS

Let $f(t)$ be a time series, and define its HS as given by equation

$$\rho_f(t, \varpi) = \frac{\left|\int_{t-D}^{t} \Psi f(\tau, \varpi) \exp(-i\varpi\tau)\mathrm{d}\tau\right|}{\sqrt{\int_{t-D}^{t} \left|\Psi f(\tau, \varpi)\right|^2 \mathrm{d}\tau \left|D\right|}}, \quad \forall t, \varpi \in R \tag{7}$$

Or

$$\gamma_f(t, \varpi) = \frac{\left|\int_{t-D}^{t} \Psi f(\tau, \varpi) \exp(-i\varpi\tau)\mathrm{d}\tau\right|}{\int_{t-D}^{t} \left|\Psi f(\tau, \varpi)\right| \mathrm{d}\tau}, \quad \forall t, \varpi \in R \tag{8}$$

where $\left|D\right|$ represents the length of the time interval D (as in Equation (6)). Here, the HS can be regarded as the complex correlation coefficient between the $z_1(t)$ and $z_2(t)$ as defined by

$$z_1(\tau) = \Psi f(\tau, \varpi);\ z_2(\tau) = \exp(i\varpi\tau) \tag{9}$$

As a result of the Inaction principle (*i.e.* NTFT's harmonic invariance), the NTFT of a time series with harmonic information will also contain this harmonic information. However, this harmonic information may not be apparent in the NTFT spectrum due to its small amplitude. The HS, on the other hand, eliminates the influence of energy on harmonic information by implementing a normalization process. Therefore, in theory, HS will highlight any harmonic information, regardless of its energy level. This is similar to the fact that a flower must bloom, regardless of its size.

Furthermore, HS exhibits strong anti-interference ability in detecting harmonic information. Interference is usually non-harmonic and therefore does not contribute significantly to the harmonic structure, making it difficult to leave a trace in the HS.

3. Simulated HS Analysis

To verify the effectiveness of HS, this paper designed a simulation experiment. In the simulation experiment, four methods, namely FT, LOFAR, NTFT, and HS, were used to analyze the simulated signal.

$$f_1(t) = \begin{cases} 5\exp\left[i\left(2\pi \cdot 140t + 10\right)\right] & t \in [12,17] \\ 0 & \text{else} \end{cases} \tag{10}$$

$$f_2(t) = \begin{cases} 5\exp\left[i\left(2\pi \cdot 150t + 20\right)\right] & t \in [6,20] \\ 0 & \text{else} \end{cases} \tag{11}$$

$$f_3(t) = \begin{cases} 5\exp\left[i\left(2\pi \cdot 160t + 5\right)\right] & t \in [5,10] \\ 0 & \text{else} \end{cases} \tag{12}$$

The simulated signal is composed of 3 complex sub-signals and strong complex Gaussian white noise. The three sub-signals, namely $f_1(t)$, $f_2(t)$, $f_3(t)$ as are shown in Equation 10-Equation 12, are single-frequency signals with different frequencies of 140 Hz, 150 Hz, and 160 Hz, and with different initial phases and different durations as well . The noise lasts for the entire sampling period with a standard deviation of 200 which make the signal-to-noise ratio (SNR) of the sub-signals to be −36.81 dB, −32.34 dB, and −36.81 dB, respectively. The sampling frequency is 4800 Hz and the total duration is 30s.

From the time-domain graph of the simulated signal (**Figure 1(a)**), no obvious signal can be seen, indicating that the signal-to-noise ratio of the signal is very low. In the FT spectrum of the simulated signal (**Figure 1(b)**), a sharp peak appears at 150 Hz, and there is no spectral leakage at this peak, indicating the presence of a single-frequency signal at 150 Hz in the simulated signal. However, there are three single-frequency signals at 140 Hz, 150 Hz, and 160 Hz in the simulated signal, and no peaks appear at 140 Hz and 160 Hz in **Figure 1(b)**, indicating that FT cannot detect these two single-frequency signals. There is no obvious single-frequency signal in the NTFT (**Figure 1(c)**). From the HS (**Figure 1(d)**), three obvious line spectra with frequencies of 140 Hz, 150 Hz, and 160 Hz

exist in the simulated signal. The time resolution of each line spectrum is still acceptable, and the duration of the line spectra can be determined from the HS. The frequency resolution of each line spectrum is high, which is represented by the thin line spectra in Figure 1(d). Combined with the simulated signal constructed by formulas (10)-(12), it can be concluded that HS can detect these three single-frequency signals.

When the signal-to-noise ratio is greater than −35 dB, both FT and HS can detect this line spectrum (150 Hz); when the signal-to-noise ratio is less than −35 dB, FT cannot detect this line spectrum (140 Hz, 160 Hz), while HS can. This indicates that HS proposed in this paper has better ability to detect weak harmonic signals than FT.

4. Underwater Acoustic Data Analysis

In order to demonstrate the harmonic signal detection capability of the HS, the present study conducted corresponding LOFAR spectrum analysis and HS analysis using passive sonar data obtained in a certain sea area of the South China Sea in 2015 (see Figure 2(a)).

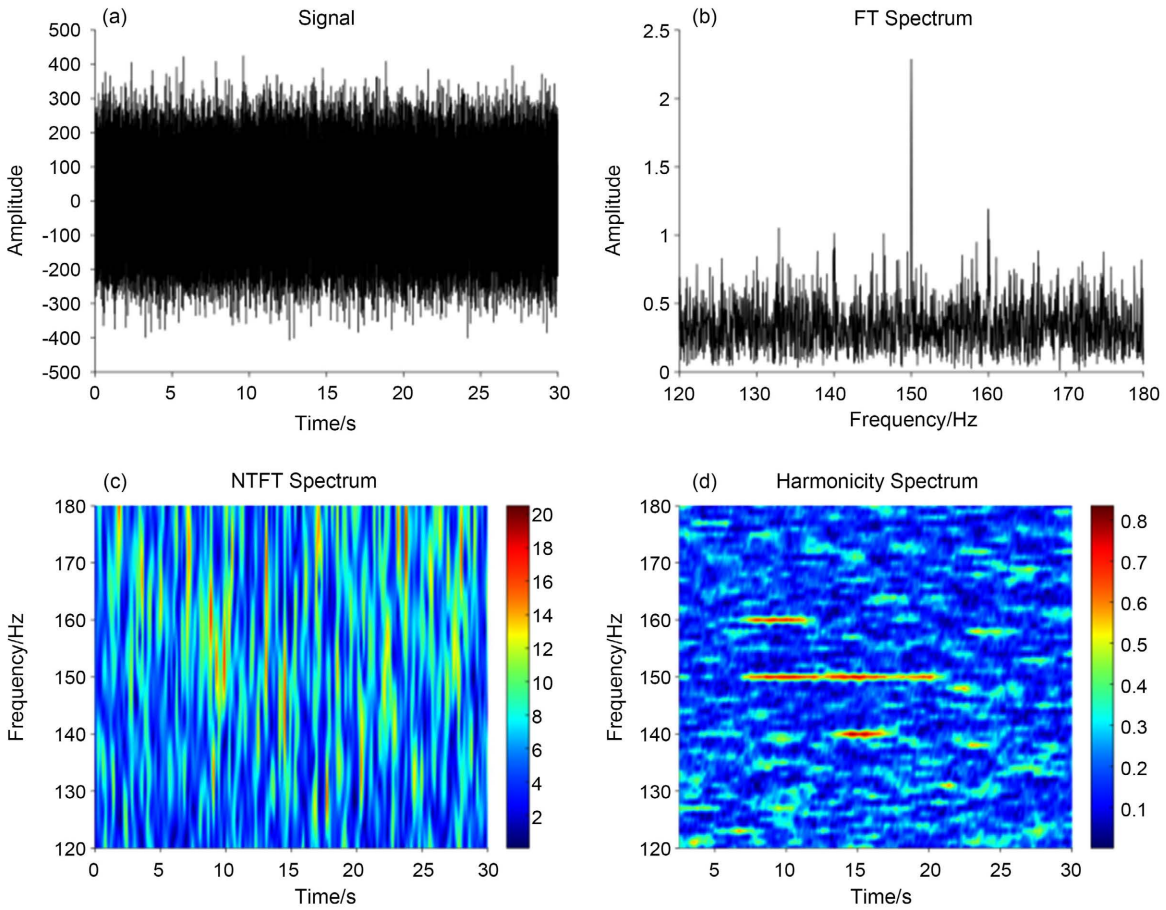

Figure 1. Analysis results of the simulated signal. (a) Represents the simulated signal; (b) represents the FT spectrum of the simulated signal; (c) represents the NTFT spectrum of the simulated signal; (d) represents the HS of the simulated signal.

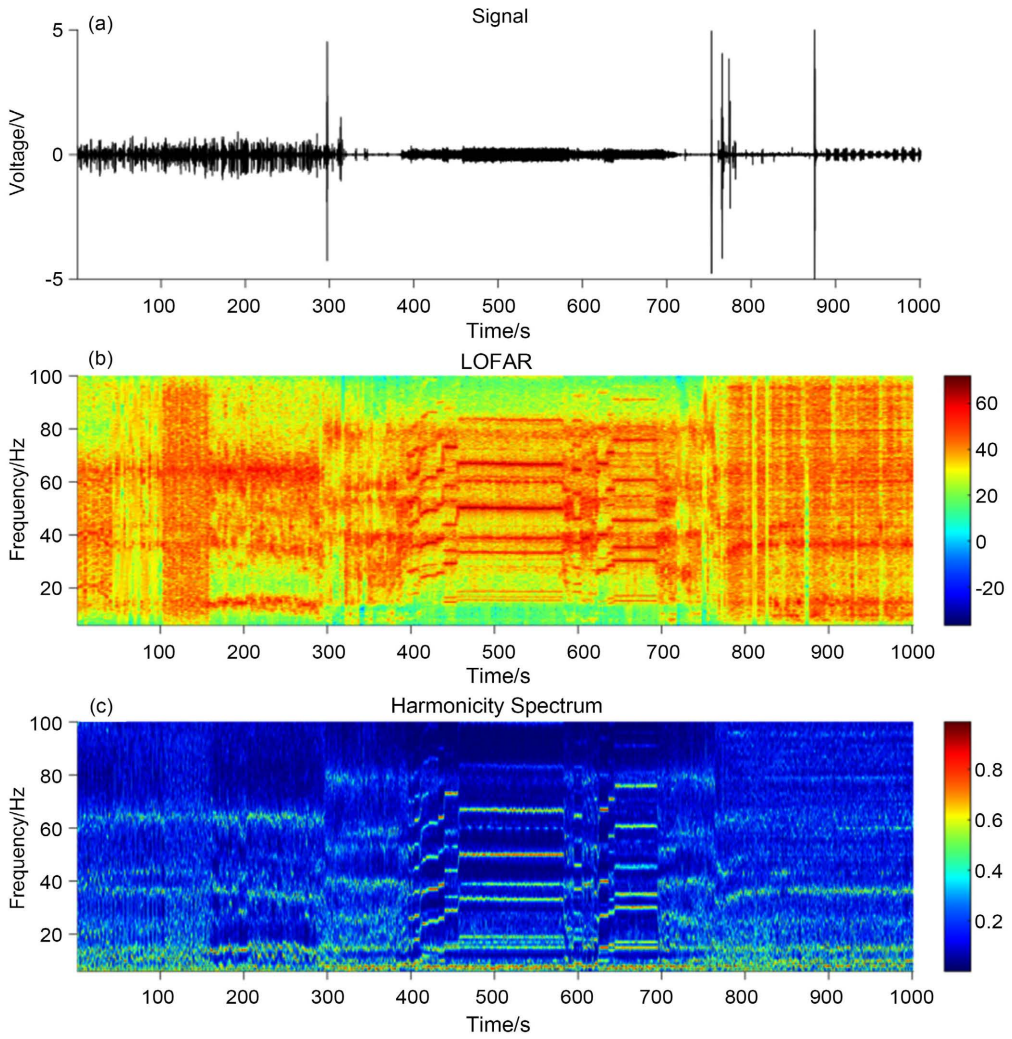

Figure 2. Results of underwater acoustic data analysis. (a) shows acoustic observation data; (b) shows LOFAR spectrum of the data; (c) shows HS of the data.

As shown in **Figure 2(b)** and **Figure 2(c)**, the HS clearly displays the temporal variation of the line spectra signal, which is more distinct compared to the LOFAR spectrum, indicating that the resolution of HS is stronger than that of LOFAR spectrum. Additionally, HS is more resistant to interference than LOFAR spectrum. The numerous vertical lines in the LOFAR plot are all caused by interference or environmental changes, while there is no such interference in HS. Furthermore, as depicted in **Figure 2(c)**, the value of the line spectra reflects the harmonic degree of the signal, and a larger HS value implies a higher possibility of the signal's existence. This ability of the HS can be used as the basis for determining whether a target exists. This ability is little affected by the environment, which is of great significance for target detection and real-time tracking.

5. Conclusion

A new spectrum called HS is developed, based on the NTFT and complex correlation coefficient. HS is capable of perceiving harmonic information in time se-

ries, especially weak harmonic information. HS has higher sensitivity than Fourier spectrum and time-frequency spectrum in detecting weak harmonic signals. In terms of the ability to perceive line spectra, HS has better resolution and anti-interference performance than LOFAR spectrum.

Conflicts of Interest

The authors declare no conflicts of interest regarding the publication of this paper.

References

[1] Fourier, J. (1807) Théorie de la propagation de la chaleur dans les solides. *Manuscrispt submitted to the Institute of France*.

[2] Gabor, D. (1946) Theory of Communication. *Journal of the Institution of Electrical Engineers—Part III: Radio and Communication*, **93**, 429-457. https://doi.org/10.1049/ji-3-2.1946.0076

[3] Morlet, J., Arens, G., Fourgeau, E. and Giard, D. (1982) Wave Propagation and Sampling Theory—Part II, Sampling Theory and Complex Waves. *Geophysics*, **47**, 222-236. https://doi.org/10.1190/1.1441329

[4] Di Martino, J.C., Haton, J.P. and Laporte, A. (1993) Lofargram Line Tracking by Multistage Decision Process. 1993 *IEEE International Conference on Acoustics, Speech, and Signal Processing*, Minneapolis, 27-30 April 1993, 317-320. https://doi.org/10.1109/ICASSP.1993.319119

[5] Wolff, S., Thomas, J. and Williams, T. (1962) The Polarity-Coincidence Correlator: A Nonparametric Detection Device. *IRE Transactions on Information Theory*, **8**, 5-9. https://doi.org/10.1109/TIT.1962.1057680

[6] Neyman, J. and Pearson, E.S. (1933) On the Problem of the Most Efficient Tests of Statistical. *Philosophical Transactions of the Royal Society of London*, **231**, 289-337. https://doi.org/10.1098/rsta.1933.0009

[7] Liu, L.T. (2007) Normal Morlet Wavelet Transform and Its Application to the Earth's Polar Motion. *Journal of Geophysical Research: Solid Earth*, **112**. https://doi.org/10.1029/2006JB004895

[8] Liu, L.T. and Hsu, H. (2012) Inversion and Normalization of Time-Frequency Transform. *Applied Mathematics & Information Sciences*, **6**, 67-74.

[9] Cai, S., Liu, L.T. and Wang, G.C. (2018) Short-Term Tidal Level Prediction Using Normal Time-Frequency Transform. *Ocean Engineering*, **156**, 489-499. https://doi.org/10.1016/j.oceaneng.2018.03.021

[10] Li, S.D., Liu, L.T., Cai, S. and Wang, G.C. (2019) Tidal Harmonic Analysis and Prediction with Least-Squares Estimation and Inaction Method. *Estuarine Coastal and Shelf Science*, **220**, 196-208. https://doi.org/10.1016/j.ecss.2019.02.047

[11] Su, X.Q., Liu, L.T., Houtse, H. and Wang, G.C. (2014) Long-Term Polar Motion Prediction Using Normal Time-Frequency Transform. *Journal of Geodesy*, **88**, 145-155. https://doi.org/10.1007/s00190-013-0675-7

[12] Duan, P.S. and Huang, C.L. (2020) Intradecadal Variations in Length of Day and Their Correspondence with Geomagnetic Jerks. *Nature Communications*, **11**, Article No. 2273. https://doi.org/10.1038/s41467-020-16109-8

[13] Wang, G.C., Liu, L.T., Xu, A. and Pan, F. (2018) On the Capabilities of the Inaction Method for Extracting the Periodic Components from GPS Clock Data. *GPS Solu-*

tion, **22**, Article No. 92. https://doi.org/10.1007/s10291-018-0757-3

[14] Zhou, Z.B., Liang, X.H., Shi, Z.M. and Wang, G.C. (2022) A New Method to Restrain Schuler Periodic Oscillation in Inertial Navigation System Based on Normal Time-Frequency Transform. *IEEE Transactions on Instrumentation and Measurement*, **71**, 1-15. https://doi.org/10.1109/TIM.2022.3170993